Event reconstruction algorithms for the ATLAS trigger

Fonseca-Martin T.[11], Abolins M.[42], Adragna P.[57], Aleksandrov E.[17], Aleksandrov I.[17], Amorim A.[36], Anderson K.[13], Anduaga X.[37], Aracena I.[62], Asquith L.[69], Avolio G.[11], Backlund S.[11], Badescu E.[9], Baines J.[58], Barria P.[61,29], Bartoldus R.[62], Batreanu S.[9,11], Beck H.P.[6], Bee C.[46], Bell P.[44], Bell W.H.[21], Bellomo M.[56], Benslama K.[59], Berge D.[11], Berger N.[34,27], Berry T.[25], Biglietti M.[52], Blair R. R.[1], Bogaerts A.[11], Bold T.[68], Bosman M.[5], Boyd J.[11], Brelier B.[48], Burckhart-Chromek D.[11], Buttar C.[21], Campanelli M.[42], Caprini M.[9], Carlino G.[52], Casadei D.[51], Casado P.[5], Cataldi G.[39], Cimino D.[28], Ciobotaru M.[9,68,11], Clements D.[21], Coccaro A.[20], Conde Muino P.[36], Conventi F.[52], Corso-Radu A.[68], Costa M.J.[70], Coura Torres R.[60], Cranfield R.[69], Cranmer K.[51], Crone G.[69], Dam M.[50], Damazio D.[4], Dawson I.[65], Dawson J.[1], De Almeida Simoes J.[40], De Cecco S.[61,29], De Santo A.[25], DellaPietra M.[52], Delsart P.-A.[48], Demers S.[62], Demirkoz B.[11], Di Mattia A.[42], Dionisi C.[61,29], Djilkibaev R.[51], Dobinson R.[11], Dobson M.[11], Dotti A.[28], Dova M.[37], Drake G.[1], Dufour M.-A.[47], Eckweiler S.[43], Ehrenfeld W.[15], Eifert T.[19], Ellis N.[11], Emeliyanov D.[58], Enoque Ferreira de Lima D.[60], Ermoline Y.[42], Eschrich I.[68], Facius K.[50], Falciano S.[29], Farthouat P.[11], Feng E.[13], Ferland J.[48], Ferrari R.[56], Ferrer M.L.[18], Fischer G.[26], Francis D.[11], Gadomski S.[6], Garitaonandia Elejabarrieta H.[5], Gaudio G.[56], Gaumer O.[19], George S.[25], Giagu S.[61,29], Goncalo R.[25], Gorini B.[11], Gorini E.[64,39], Gowdy S.[62], Grabowska-Bold I.[11], Grancagnolo S.[64,39], Green B.[25], Haas S.[11], Haberichter W.[1], Hadavand H.[63], Haeberli C.[6], Haller J.[23,15], Hamilton A.[19], Hansen J.R.[50], Hauschild M.[11], Hauser R.[42], Head S.[44], Hillier S.[7], Hoecker A.[11], Hryn'ova T.[11], Hughes-Jones R.[44], Huston J.[42], Idarraga J.[48], Igonkina O.[54], Inada M.[33], Jain V.[30], Johns K.[3], Joos M.[11], Kama S.[15], Kanaya N.[33], Kazarov A.[55], Kehoe R.[63], Khoriauli G.[59], Kieft G.[53], Kilvington G.[25], Kirk J.[58], Kiyamura H.[33], Kolos S.[68], Kono T.[11], Konstantinidis N.[69], Korcyl K.[14], Kordas K.[6], Kotov V.[17], Krasznahorkay A.[11,16], Kubota T.[67], Kugel A.[45], Kuhn D.[31], Kurasige H.[33], Kuwabara T.[67], Kwee R.[74], Lankford A.[68], LeCompte T.[1], Leahu L.[9,11], Leahu M.[9], Ledroit F.[22], Lehmann Miotto G.[11], Lei X.[3], Lellouch D.[72], Leyton M.[35], Li S.[15], Lim H.[1], Lohse T.[26], Losada M.[8], Luci C.[61,29], Luminari L.[29], Mapelli L.[11], Martin B.[11], Martin B.T.[42], Marzano F.[29], Masik J.[44], McMahon T.[25], Mcpherson R.[71], Medinnis M.[15], Meessen C.[46], Meirosu C.[9], Messina A.[11], Mincer A.[51], Mineev M.[17], Misiejuk A.[25], Moenig K.[74], Monticelli F.[37], Moraes A.[4], Moreno D.[8], Morettini

Work supported in part by US Department of Energy contract DE-AC02-76SF00515.

SLAC National Accelerator Laboratory, Menlo Park, CA 94025

P.[20], Murillo Garcia R.[11], Nagano K.[32], Nagasaka Y.[24], Negri A.[68], Nemethy P.[51], Neusiedl A.[43], Nisati A.[61,29], Nozicka M.[15], Omachi C.[33], Osculati B.[20], Osuna C.[5], Padilla C.[11], Panikashvili N.[66], Parodi F.[20], Pasqualucci E.[61,29], Pauly T.[11], Perera V.[58], Perez E.[5], Perez Reale V.[11], Petersen J.[11], Piegaia R.[10], Pilcher J.[13], Pinzon G.[8], Pope B.[42], Potter C.[47], Primavera M.[39], Radescu V.[15], Rajagopalan S.[4], Renkel P.[63], Rescigno M.[61], Rieke S.[43], Risler C.[26], Riu I.[5], Robertson S.[47], Roda C.[28], Rodriguez D.[8], Rogriquez Y.[8], Ryabov Y.[55], Ryan P.[42], Salvatore D.[12], Santamarina C.[47], Santamarina Rios C.[47], Scannicchio D.[56], Scannicchio D.A.[56], Schiavi C.[20], Schlereth J.[1], Scholtes I.[11], Schooltz D.[42], Scott W.[58], Segura E.[5], Shimbo N.[33], Sidoti A.[29], Siragusa G.[64,39], Sivoklokov S.[49], Sloper J.E.[11], Smizanska M.[38], Soloviev I.[11], Soluk R.[2], Spagnolo S.[64,39], Spiwoks R.[11], Stancu S.[9,68,11], Steinberg P.[4], Stelzer J.[11], Stradling A.[73], Strom D.[54], Strong J.[25], Su D.[62], Sushkov S.[5], Sutton M.[69], Szymocha T.[14], Tapprogge S.[43], Tarem S.[66], Tarem Z.[66], Teixeira-Dias P.[25], Tokoshuku K.[32], Torrence E.[54], Touchard F.[46], Tremblet L.[11], Tripiana M.[37], Usai G.[13], Vachon B.[47], Vandelli W.[11], Ventura A.[39], Vercesi V.[56], Vermeulen J.[53], Von Der Schmitt J.[41], Wang M.[59], Watson A.[7], Wengler T.[44], Werner P.[11], Wheeler-Ellis S.[68], Wickens F.[58], Wiedenmann W.[73], Wielers M.[58], Wilkens H.[11], Winklmeier F.[11], Woehrling E.-E.[7], Wu S.-L.[73], Wu X.[19], Xella S.[50], Yamazaki Y.[32], Yu M.[45], Zema F.[11], Zhang J.[1], Zhao L.[51], Zobernig H.[73], dos Anjos A.[73], zur Nedden M.[26], zcan E.[69] and nel G.[68,11].

[1] Argonne National Laboratory, Argonne, Illinois
[2] University of Alberta, Edmonton
[3] University of Arizona, Tucson, Arizona
[4] Brookhaven National Laboratory (BNL), Upton, New York
[5] Institut de Fsica d'Altes Energies (IFAE), Universitat Autnoma de Barcelona, Bellaterra (Barcelona)
[6] Laboratory for High Energy Physics, University of Bern, Bern
[7] School of Physics and Astronomy, The University of Birmingham, Birmingham
[8] Universidad Antonio Narino, Bogot, Colmbia
[9] National Institute for Physics and Nuclear Engineering, Institute of Atomic Physics, Bucharest
[10] Univerity of Buenos Aires, Buenos Aires
[11] European Laboratory for Particle Physics (CERN), Geneva
[12] Dipartimento di Fisica dell' Universit della Calabria e I.N.F.N., Cosenza
[13] University of Chicago, Enrico Fermi Institute, Chicago, Illinois
[14] Institute of Nuclear Physics, Polish Academy of Sciences, Cracow
[15] Deutsches Elektronen-Synchrotron (DESY), Hamburg
[16] University of Debrecen ***
[17] Joint Institute for Nuclear Research, Dubna
[18] Laboratori Nazionali di Frascati dell' I.N.F.N., Frascati
[19] Section de Physique, Universit de Genve, Geneva
[20] Dipartimento di Fisica dell' Universit di Genova e I.N.F.N., Genova
[21] Department of Physics and Astronomy, University of Glasgow, Glasgow
[22] Laboratoire de Physique Subatomique et de Cosmologie de Grenoble (LPSC), IN2P3-CNRS-Universit Joseph Fourier, Grenoble
[23] University of Hamburg, Germany ***

[24] Hiroshima Institute of Technology, Hiroshima
[25] Department of Physics, Royal Holloway and Bedford New College, Egham
[26] Institut fr Physik, Humboldt Universitt, Berlin
[27] Institut National de Physique Nucleaire et de Physique des Particules
[28] Dipartimento di Fisica dell' Universit di Pisa e I.N.F.N., Pisa
[29] I.N.F.N. Roma
[30] Indiana University, Bloomington, Indiana
[31] Institut fr Experimentalphysik der Leopold-Franzens-Universitt Innsbruck, Innsbruck
[32] KEK, High Energy Accelerator Research Organisation, Tsukuba
[33] Kobe University, Kobe
[34] Laboratoire d'Annecy-le-Vieux de Physique des Particules (LAPP), IN2P3-CNRS, Annecy-le-Vieux
[35] Lawrence Berkeley Laboratory and University of California, Berkeley, California
[36] Laboratorio de Instrumentacao e Fisica Experimental, Lisboa
[37] National University of La Plata, La Plata
[38] Department of Physics, Lancaster University, Lancaster
[39] Dipartimento di Fisica dell' Universit di Lecce e I.N.F.N., Lecce
[40] University Catlica-Figueira da Foz and University Nova de Lisboa, Lisbon
[41] Max-Planck-Institut fr Physik, Mnchen
[42] Michigan State University, Department of Physics and Astronomy, East Lansing, Michigan
[43] Institut fr Physik, Universitt Mainz, Mainz
[44] Department of Physics and Astronomy, University of Manchester, Manchester
[45] Lehrstuhl fr Informatik V, Universitt Mannheim, Mannheim
[46] Centre de Physique des Particules de Marseille, IN2P3-CNRS, Marseille
[47] Department of Physics, McGill University, Montreal
[48] University of Montreal, Montreal
[49] Moscow State University, Moscow
[50] Niels Bohr Institute, University of Copenhagen, Copenhagen
[51] Department of Physics, New York University, New York
[52] Dipartimento di Scienze Fisiche, Universit di Napoli 'Federico II' e I.N.F.N., Napoli
[53] FOM - Institute SAF NIKHEF and University of Amsterdam/NIKHEF, Amsterdam
[54] University of Oregon, Eugene, Oregon
[55] Petersburg Nuclear Physics Institute (PNPI), St. Petersburg
[56] Dipartimento di Fisica Nucleare e Teorica dell' Universit di Pavia e I.N.F.N., Pavia
[57] Department of Physics, Queen Mary and Westfield College, University of London, London
[58] Rutherford Appleton Laboratory, Chilton, Didcot
[59] University of Regina, Regina
[60] Universidade Federal do Rio de Janeiro, COPPE/EE/IF, Rio de Janeiro
[61] Dipartimento di Fisica dell' Universit di Roma I 'La Sapienza'
[62] Stanford Linear Accelerator Center (SLAC), Stanford
[63] Department of Physics, Southern Methodist University, Dallas, Texas
[64] Universit degli Studi del Salento ***
[65] Department of Physics, University of Sheffield, Sheffield
[66] Department of Physics, Technion, Haifa
[67] International Center for Elementary Particle Physics, University of Tokyo, Tokyo
[68] University of California, Irvine, California
[69] Department of Physics and Astronomy, University College London, London
[70] Instituto de Fisica Corpuscular (IFIC) Universidad de Valencia
[71] University of Victoria, Victoria
[72] Department of Particle Physics, The Weizmann Institute of Science, Rehovot

[73] Department of Physics, University of Wisconsin, Madison, Wisconsin
[74] Deutsches Elektronen-Synchrotron (DESY), Zeuthen

E-mail: Teresa.Fonseca.Martin@cern.ch

Abstract. The ATLAS experiment under construction at CERN is due to begin operation at the end of 2007. The detector will record the results of proton-proton collisions at a center-of-mass energy of 14 TeV. The trigger is a three-tier system designed to identify in real-time potentially interesting events that are then saved for detailed offline analysis. The trigger system will select approximately 200 Hz of potentially interesting events out of the 40 MHz bunch-crossing rate (with 10^9 interactions per second at the nominal luminosity).

Algorithms used in the trigger system to identify different event features of interest will be described, as well as their expected performance in terms of selection efficiency, background rejection and computation time per event. The talk will concentrate on recent improvements and on performance studies, using a very detailed simulation of the ATLAS detector and electronics chain that emulates the raw data as it will appear at the input to the trigger system.

1. Introduction

ATLAS is a general purpose particle physics detector which is described in detail in [1]. It will detect proton-proton collisions in the Large Hadron Collider (LHC). Its primary goals are to understand the mechanism for electroweak symmetry breaking and to search for new physics beyond the Standard Model. The LHC is expected to start its operation next spring. It will eventually provide proton-proton collisions at a center of mass energy of about 14 TeV, a design luminosity of $10^{34} cm^{-2} s^{-1}$ and a bunch-crossing rate of 40MHz. For every bunch intersection around 23 inelastic proton-proton interactions are expected. This means about 10^9 interactions per second. The limits on our capability to store data and the expected event size give an upper limit of $200 Hz$ to the trigger output. ATLAS trigger is expected to have a rejection power of $\sim 10^6$ while being the trigger efficiency as high as possible for the interesting events.

ATLAS trigger is structured in three levels. The First Level (LVL1) uses custom built electronics. It reduces the trigger rate in 3 orders of magnitude, giving a response in less than $2.5 \mu s$ It receives coarse data from the Calorimeter and muon subdetectors. The so-called High Level Trigger (HLT) is software-based, it is composed by a Second Level Trigger (LVL2) and a third level trigger called Event Filter (EF). LVL2 has access to the full detector granularity data inside a Region of Interest (RoI) that has been defined by LVL1 and whose position is improved using LVL2 data as soon as available. LVL2 uses algorithms specifically written for the trigger to accomplish the hard speed limits required at this level. The EF has as well access to the full detector granularity, it uses as a seed the RoI provided by LVL2, though it has potential access to the full event reconstruction. EF uses offline reconstruction algorithms as much as possible in the online trigger environment.

ATLAS trigger has been designed according to two basic concepts:

- Use of Regions of Interest (RoI). LVL1 identifies interesting trigger objects and provides its η and ϕ coordinates. A finite detector volume is defined around these *eta* and *phi* coordinates, this is the so-called Region of Interest (RoI). In the following steps of the trigger chain only these subsamples of the subdetectors data are used. RoIs are used to speed up the trigger process.
- Early rejection. Trigger signatures are evaluated after the execution of each algorithm, as soon as the trigger requirements are not satisfied the processing of the trigger signature is interrupted. If all the trigger signatures (that are being processed in parallel) have been interrupted, the event is rejected immediately.

These two basic concepts are discussed in more detail in the following references: [1] and [2]

In this paper we will first give a brief description on how the ATLAS trigger menus are defined. Then there will be a separate section for each of the main trigger objects. The first of these sections, devoted to the egamma object will be explained with some detail, this should give a general idea for all the other trigger objects since the basic concepts are common to all of them. In the remaining sections a brief description of the corresponding trigger slice will be given together with a couple of examples of performance results.

B-physics slice is not covered in this paper since it is being covered in [3].

2. ATLAS Trigger Menu

The ATLAS trigger menus are built based in elemental trigger objects as: electrons, photons, taus, muons, jets, b-tagged jets, B-physics objects, missing transverse energy (E_T), etc. Each of these basic objects are defined using a chain of algorithms that are executed sequentially. The algorithms are grouped in two big families (for details see Ref. [2]):

- Feature Extraction (FEX) Algorithms build objects as Calorimeter clusters, tracks, etc. They do not reject any event.
- Hypothesis Algorithms perform the selection applying cuts on the objects built by the FEX. The execution of a chain is stopped when a hypothesis algorithm is not satisfied, and the event would be rejected unless it has successfully pass the selection in some other chain.

Such a chain of algorithms that defines a trigger object is called a "slice". Typically there is a FEX algorithm followed by a hypothesis algorithm. For a given slice the threshold values used to define the cuts are programmable. A particular set of cuts define a "signature", for example, we have a signature named "e25i" this corresponds to an electron with a transverse energy above 25 GeV that satisfies the isolation criteria at LVL1; another signature is named "e15" this corresponds to an electron with a transverse energy above 15 GeV. For each of the basic trigger objects mentioned above exist several different signatures corresponding to different cut thresholds of the selection variables. Typically each signature corresponds to a different threshold in the transverse energy.

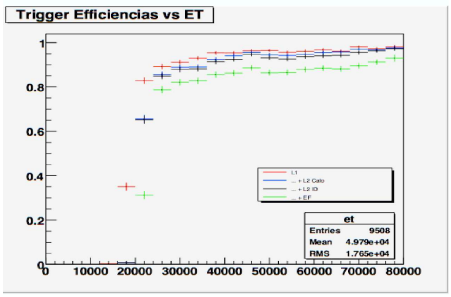

Figure 1. Turn on curve for the e25i signature of the electron trigger.

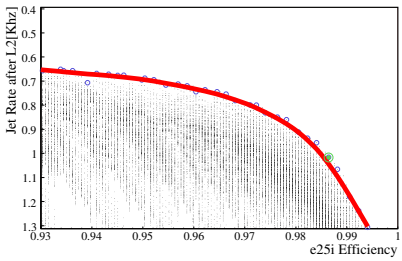

Figure 2. Example of e25i signature optimization.

Trigger signatures are also formed requesting simultaneously several of the previous objects, for example: ($e15i$ & missing E_T), ($e15i$ & $tau25i$), etc. Combining all these different signatures a Trigger Menu is built according to the physics goals and the limitations imposed by the event rates.

3. Egamma Trigger Slice

The electron and photon trigger slices share the feature extraction (FEX) algorithms that built the Calorimeter cluster and shower shape variables. Then for all the electron and photon signatures the caching mechanism is used for the Calorimeter FEX algorithms, this mechanism guarantees that a FEX algorithm is not executed more than once seeded by the same trigger object, instead of executing it again it retrieves and copies the result from the first execution, saving computation time, for detailed description on this mechanism see Ref. [2]. The main difference among the electron and photon slices is that in the first one data from Inner Detector is used to reconstruct tracks both at LVL2 and EF, and these tracks are matched in η, ϕ and E_T/p_T with the Calorimeter clusters.

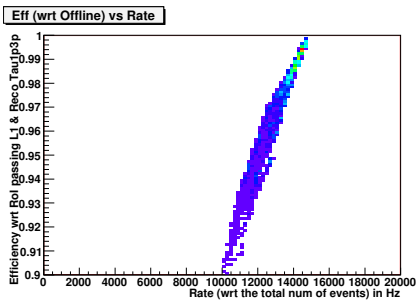

Figure 3. Example of tau trigger optimization at LVL2.

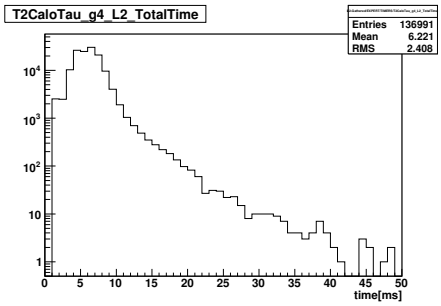

Figure 4. Execution time for LVL2 Calorimeter reconstruction in the Tau trigger measured during May Technical Run.

The electron and photon slices are composed by the following chain of algorithms:

- T2CaloEgamma: performs Calorimeter cluster reconstruction using full detector granularity and computes shower shape variables that are used to discriminate electrons and photons mainly from jets.
- L2PhotonFEX (only for photon slice): builds a LVL2 photon object.
- L2CaloHypo: performs LVL2 selection cuts using Calorimeter cluster and shower shape variables.
- L2Tracking (only for electron slice): reconstructs LVL2 tracks using Inner Detector information. Currently two alternative tracking algorithms are implemented, they are called IDSCAN and SiTrack. The steps followed for track reconstruction in IDSCAN are:
  (1) zFinder: Reconstruction of the z-position of the primary pp collision.
  (2) hitFilter & groupCleaner: The main pattern recognition step.
  (3) trackFitter: final track fit and removal of outliers.

  The steps followed in SiTrack can be summarized as:
  (1) Space point sorting.
  (2) Track seeds formation.
  (3) Primary vertex reconstruction.
  (4) Track extension.
- L2ElectronFEX (only electrons): builds a LVL2 electron object performing a match among all the available Calorimeter clusters and tracks.
- L2CaloIDHypo (only electrons): performs selection cuts on track-cluster matching variables.
- TrigCaloRec: reconstructs EF Calorimeter clusters, it wraps-up offline tools.

- EF IDTrack (only for electrons): reconstructs EF tracks using Inner Detector (ID) information. These algorithms are based on offline tools.
- EFTrackHypo (only for electrons): applies selection cuts on EF tracks.
- TrigEgammaRec: reconstructs egamma objects combining Calorimeter and Inner Detector information. It allows the possibility to run bremsstrahlung corrections. It wraps offline algorithms and the egamma object built is an offline object.
- TrigEFEgammaHypo: applies selection cuts on EF egamma objects. It uses Calorimeter cluster energy and other shower shape variables, and, for the electron case, track variables and cluster-track matching variables as well.

Trigger performance studies are carried out systematically. Typically the trigger efficiency and trigger rate dependency on the threshold value chosen for a selection cut is studied for each of the selection variables, as well as for η and ϕ positions. To estimate the trigger rates di-jets samples are used. Trigger efficiency for signal is studied using several full MonteCarlo (MC) simulations (including detailed realistic description of the detector using Geant 4), among the more characteristic ones are: single electrons and single photons of a particular transverse energy value (ex: 10 GeV, 20 GeV, 60 GeV, 100 GeV) and corresponding to an energy scan from 7 GeV to 80 GeV, $Z \rightarrow e^+e^-$, $W \rightarrow e\nu$ $H \rightarrow \gamma\gamma$ with and without pile-up effects. Other Standard Model, SUSY and exotic samples are studied, all these are compared to understand and crosscheck the trigger efficiency.

For example in Figure 1 we can see the trigger efficiency turn on curve for the *e25i* signature (electron with transverse energy higher than 25 GeV) as a function of the transverse energy of the electron for the different trigger levels: LVL1, LVL2 cuts based on Calorimeter variables, LVL2 cuts based on Calorimeter cluster and track matching and EF. This study corresponds to a sample of single electrons with transverse energy between 7 GeV and 80 GeV.

The thresholds applied in the selection cuts are currently optimized using MC full simulation, studying trigger efficiency for signal samples and trigger rates for background and signal samples. This study consists on the variation of the threshold cut within a given range for all the variables involved in the selection, and the computation of the corresponding trigger efficiencies and rates. Such a study is shown in Figure 2 in which each of the dots in the plot represents a different set of threshold values for the LVL2 Calorimeter selection variables (there are four selection variables currently being used E_T and shower shape variables including leakage in the hadronic Calorimeter) we can read the corresponding trigger efficiency on the X axis, and the trigger rate on the Y axis. From this plot it can be extracted the higher trigger efficiency that can be obtained for a given rate or the lowest rate for a given trigger efficiency, in a separate file are kept the cut thresholds that correspond to each of these points. This plot corresponds to a signal sample of single electrons of 25 GeV transverse energy and a di-jet sample of more than 17GeV transverse energy.

4. Tau Trigger Slice

The tau trigger slice structure is very similar to the electron one. The FEX algorithms that built the Calorimeter clusters and the Inner Detector tracks are mainly the same than for the electron case though some of the reconstruction programmable parameters are different in both cases (when this is the case, caching mechanism can not be used). The tau slice is formed by a sequence of algorithms that perform the following functions:

- Build a LVL2 Calorimeter cluster and compute corresponding shower shape variables.
- Perform selection cuts on Calorimeter variables.
- Reconstruct a LVL2 Inner Detector track.
- Apply selection requirements on track parameters.

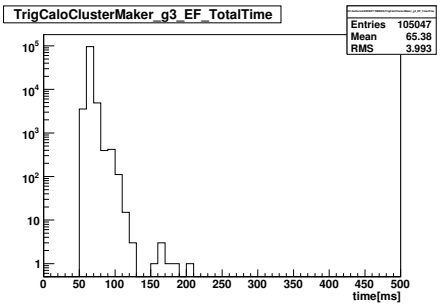

Figure 5. Execution time for algorithm building Calorimeter clusters at EF measured during May Technical Run.

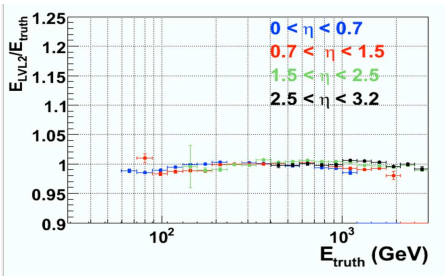

Figure 6. Energy scale resolution for L2 jet algorithm.

- Reconstruct a LVL2 tau object.
- Apply selection, including cluster-track matching, to the LVL2 tau object.
- Reconstruct EF Calorimeter cluster.
- Reconstruct EF Inner Detector tracks.
- Build EF tau object.
- Apply selection cuts to EF tau object.

In Figure 4 we have an example on time performance for the algorithm that reconstructs the LVL2 Calorimeter cluster. In Figure 3 the results for an optimization of the LVL2 Calorimeter cuts (transverse energy and shower shape variables, in this case different from the egamma ones) performed as explained in Section 3.

5. Jet Trigger Slice

The jet slice uses only Calorimeter information. The jet slice is integrated by the following sequence of algorithms:

- T2CaloJet: retrieves Calorimeter cells in the trigger RoI, runs a fast cone algorithm for jet reconstruction and calibrates the jet.
- L2JetHypo: applies a transverse energy selection cut.
- EFCaloJet: retrieves Calorimeter cells, builds Calorimeter towers and reconstructs jets wrapping offline tools.
- EFJetHypo: applies a transverse energy selection cut.

A key point in the jet slice is the jet calibration. For example in Figure 6 the energy scale resolution for LVL2 jet algorithm is shown. We can see the jet energy at LVL2 after calibration compared to the true energy of the MC simulation as a function of the true MC energy for different regions in η. A detailed description of the LVL2 jet trigger can be found in [4].

6. b-tagging

Currently there are two b-tagging trigger signatures implemented, one of them requires at least 3 jets being at least two of them tagged as b, and the other requires at least 4 jets being at least two of them identified as b jets. Only tracking information is used at LVL2 and EF. For both LVL2 and EF selection is applied through likelihood based on impact parameter. The significance of the longitudinal impact parameter is shown in Figure 7 for both signal and background. In Figure 8 the rejection for u-jets versus b-tag trigger efficiency is presented.

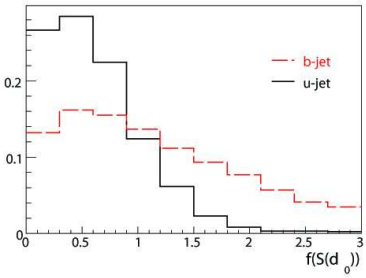

Figure 7. Significance of longitudinal impact parameter for b-jets and u-jets.

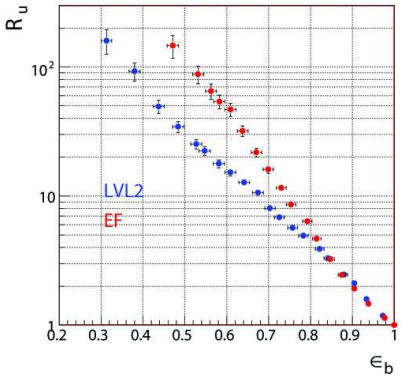

Figure 8. Rejection factor for background from u-jets versus b-tagging trigger efficiency.

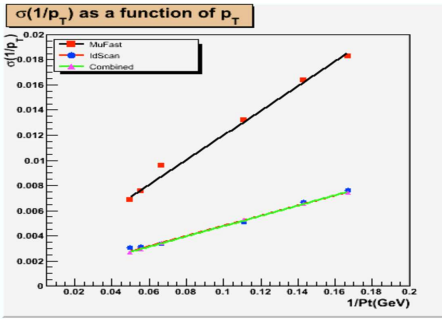

Figure 9. Transverse momentum resolution at LVL2 for muons in the barrel region.

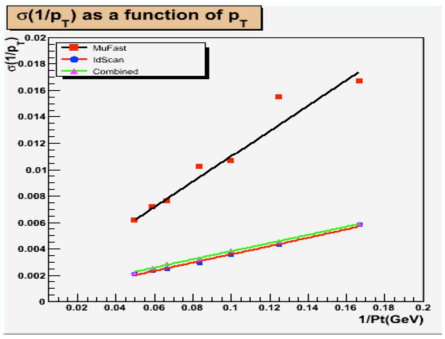

Figure 10. Transverse momentum resolution at LVL2 for muons in the End Cap region.

7. Muon Trigger Slice

The muon trigger slice relies on the information coming from the Muon Spectrometer that is complemented with the Inner Detector. The possibility of using Calorimeter information to identified isolated muons is currently under study. The following FEX algorithms are part of the muon trigger slice:

- muFast: LVL2 Muon Spectrometer stand alone track reconstruction.
- muComb: refines muon tracks combining them with the Inner Detector LVL2 information.
- muIso: Calorimeter isolation algorithm to reject muons from beauty and charm semileptonic decays.
- TrigMoore: reconstructs EF muon objects wrapping offline tools. A Muon Spectometer stand alone track reconstruction is performed, in a second step the track reconstruction is improved using the Inner Detector information.

Each FEX algorithm is followed by a hypothesis algorithm applying a selection on the corresponding track.

In Figure 9 and Figure 10 it can be observed the resolution of the inverse of the transverse momentum as a function of the inverse of the transverse momentum for the Muon Spectrometer

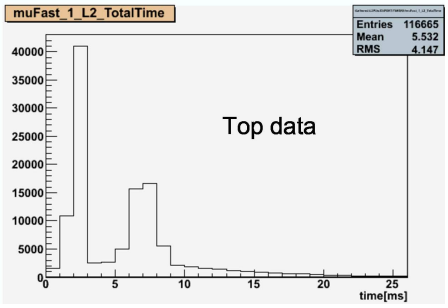

Figure 11. Execution time for LVL2 muon algorithm measured during May Technical Run.

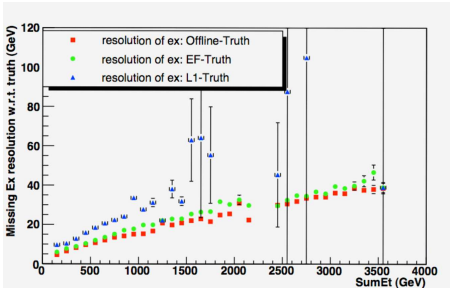

Figure 12. Missing E_T distribution.

Barrel and End-Cap regions. It can be seen the resolution for the Inner Detector stand alone tracking reconstruction, for the Muon Spectrometer stand alone tracking reconstruction, that is significantly worse, and for the Muon Spectrometer combined with Inner Detector (ID) tracking reconstruction which recovers the stand alone ID resolution.

In Figure 11 there is an example of the time performance for LVL2 stand alone Muon Spectrometer reconstruction.

8. Missing transverse energy

Missing E_T is an special slice because the RoI concept does not apply to a global quantity. To perform the missing E_T computation data preparation is a major concern since the entire Calorimeter needs to be accessed. At LVL2 all LVL2 reconstructed muons are subtracted from the missing E_T computed at LVL1. At EF the current algorithm loops over all cells in the Electro Magnetic Calorimeter. Currently is under study a new algorithm that loops over the E_x/E_y sums in the Front End Buffer header, this increases significantly the time performance but the energy resolution is reduced. All the EF reconstructed muons are taken into account for the missing E_T determination, as well as a simple hadronic calibration.

The missing E_x resolution with respect to MonteCarlo truth variable is shown in Figure 12 as a function of the transverse energy for offline reconstruction, EF and LVL1.

9. Conclusions

The ATLAS High Level Trigger (HLT) event reconstruction is mature, it is on a good track to have a successful startup. ATLAS HLT allows a sophisticated and fast event reconstruction using full detector granularity. Anyhow continuous work is ongoing to improve performance and to implement more and more complex menus.

Acknowledgments

Acknowledgments The authors would like to acknowledge the collaboration and support of ATLAS experiment in general, and its T/DAQ and software projects in particular.

References

[1] Jenni, P et al 1999 ATLAS detector and physics performance Technical Design Report, *ser. Technical Design Report ATLAS* (Geneva: CERN)
[2] George, S *et all* 2007 The ATLAS High Level Trigger Steering *in these proceedings.*
[3] Emeliyanov, D *et all* 2007 Trigger Selection Software for Beauty physics in ATLAS *in these proceedings.*
[4] Conde Muíño, P *et all* 2007 Implementation and Performance of the ATLAS Second Level Jet Trigger *in these proceedings.*